Exploration of the Transition from the Hydrodynamiclike to the Strongly Kinetic Regime in Shock-Driven Implosions

M. J. Rosenberg,[1,*] H. G. Rinderknecht,[1] N. M. Hoffman,[2] P. A. Amendt,[3] S. Atzeni,[4] A. B. Zylstra,[1] C. K. Li,[1] F. H. Séguin,[1] H. Sio,[1] M. Gatu Johnson,[1] J. A. Frenje,[1] R. D. Petrasso,[1] V. Yu. Glebov,[5] C. Stoeckl,[5] W. Seka,[5] F. J. Marshall,[5] J. A. Delettrez,[5] T. C. Sangster,[5] R. Betti,[5] V. N. Goncharov,[5] D. D. Meyerhofer,[5] S. Skupsky,[5] C. Bellei,[3] J. Pino,[3] S. C. Wilks,[3] G. Kagan,[2] K. Molvig,[2] and A. Nikroo[6]

[1]*Plasma Science and Fusion Center, Massachusetts Institute of Technology, Cambridge, Massachusetts 02139, USA*
[2]*Los Alamos National Laboratory, Los Alamos, New Mexico 87545, USA*
[3]*Lawrence Livermore National Laboratory, Livermore, California 94550, USA*
[4]*Dipartimento SBAI, Università di Roma "La Sapienza", Via A Scarpa, 14–16, I-00161 Roma, Italy*
[5]*Laboratory for Laser Energetics, University of Rochester, Rochester, New York 14623, USA*
[6]*General Atomics, San Diego, California 92186, USA*

(Received 1 November 2013; published 5 May 2014)

Clear evidence of the transition from hydrodynamiclike to strongly kinetic shock-driven implosions is, for the first time, revealed and quantitatively assessed. Implosions with a range of initial equimolar D^3He gas densities show that as the density is decreased, hydrodynamic simulations strongly diverge from and increasingly overpredict the observed nuclear yields, from a factor of ~2 at 3.1 mg/cm^3 to a factor of 100 at 0.14 mg/cm^3. (The corresponding Knudsen number, the ratio of ion mean-free path to minimum shell radius, varied from 0.3 to 9; similarly, the ratio of fusion burn duration to ion diffusion time, another figure of merit of kinetic effects, varied from 0.3 to 14.) This result is shown to be unrelated to the effects of hydrodynamic mix. As a first step to garner insight into this transition, a reduced ion kinetic (RIK) model that includes gradient-diffusion and loss-term approximations to several transport processes was implemented within the framework of a one-dimensional radiation-transport code. After empirical calibration, the RIK simulations reproduce the observed yield trends, largely as a result of ion diffusion and the depletion of the reacting tail ions.

DOI: 10.1103/PhysRevLett.112.185001 PACS numbers: 52.57.-z, 24.10.Nz, 52.35.Tc

Inertial confinement fusion implosions, whether for ignition [1] or nonignition [2,3] experiments, are nearly exclusively modeled as hydrodynamic in nature with a single average-ion fluid and fluid electrons [4,5]. However, in the early phase of virtually all inertial fusion implosions, strong shocks are launched into the capsule where they increase in strength and speed as they converge to the center and abruptly and significantly increase the ion temperature in the central plasma region. In this process, and in the rebound of the shock from the center, which initiates a burst of fusion reactions (i.e., the fusion shock burn or shock flash [6]), the mean-free path for ion-ion collisions can become, especially for lower-density fueled implosions, sufficiently long that both the shock front itself and the resulting central plasma are inadequately described by hydrodynamic modeling. This process and the transition of regimes from hydrodynamiclike to strongly kinetic are the focus of this Letter.

Recent kinetic and multiple-ion-fluid simulations have begun to explore deviations from average-ion hydrodynamic models, particularly during the shock phase of implosions when such effects are potentially paramount. For example, in an effort to explain observed yield anomalies in multiple-ion fuels of D^3He, DT, and DT^3He [7–9], researchers have investigated multiple-ion-fluid effects [10–12] as well as utilized a hybrid fluid-kinetic model [13,14]. Other modeling work has included ion viscosity and nonlocal ion transport [15] in order to reduce discrepancies with shock-generated nuclear yields. Very recently, a model for Knudsen layer losses of energetic ions [16], based in part on earlier work [17], was explored for a variety of plastic capsule implosions with relatively thick walls, all largely ablatively driven (not shock driven) and with THD fuel. In their work, the inclusion of non-Maxwellian effects and a turbulent mix model brought their simulated yields into better agreement with measurements.

In contrast to previous studies, this work represents a comprehensive experimental effort to isolate and carefully explore ion kinetic effects in shock-driven implosions by systematically varying the ion-ion mean-free path relative to the minimum shell radius, i.e., from a regime where the hydrodynamic description is approximately valid to one where it is strongly violated. To achieve this goal, this experimental campaign used virtually identical glass capsules and laser drive conditions, varied only the fill density of equimolar D^3He (from 3.1 to 0.14 mg/cm^3), and made the most comprehensive set of diagnostic

TABLE I. Key hydro-kinetic parameters, all inferred from measured quantities, in the hydrodynamiclike and strongly kinetic regimes, including the initial gas density, the yield-averaged ion temperature, the average ion-ion mean-free path at bang time, the minimum shell radius, the Knudsen number, the DD (D^3He) burn duration, the D (^3He) ion diffusion time, and the ratio of DD (D^3He) burn duration to D (^3He) diffusion time.

Initial gas density (mg/cm^3)	$\langle T_i \rangle$ (keV)	λ_{ii} (μm)	R_{shell} (μm)	N_K	$\tau_{\text{burn,DD}}$ ($\tau_{\text{burn,D}^3\text{He}}$) (ps)	$\tau_{\text{diff,D}}$ ($\tau_{\text{diff,}^3\text{He}}$) (ps)	$R_{\tau,\text{DD}}$ ($R_{\tau,\text{D}^3\text{He}}$)
3.1	14	~40	~130	~0.3	~200 (~160)	~600 (~2400)	~0.3 (~0.07)
0.14	28	~800	~85	~9	~140[a] (~120)	~10 (~40)	~14 (~3)

[a]The DD burn duration was not directly measured on this experiment but is reasonably assumed to be ~20% longer than the D^3He burn duration, based on $\tau_{\text{burn,DD}}/\tau_{\text{burn,D}^3\text{He}} \sim 1.2$ at other fill densities.

measurements possible so as to achieve the most credible hydro-kinetic parameters and to allow, in the future, the highest-fidelity comparison to simulations. The experimental measurements include absolute yields for both DD and D^3He reactions

$$D + D \rightarrow {}^3\text{He}(0.82\ \text{MeV}) + n(2.45\ \text{MeV}), \quad (1)$$

$$D + {}^3\text{He} \rightarrow \alpha(3.6\ \text{MeV}) + p(14.7\ \text{MeV}), \quad (2)$$

burn-averaged ion temperatures (T_i) for both DD and D^3He reactions, scattered light from the implosion drive, x-ray images of the imploding capsule for determination of the convergence (and the minimum shell radius), secondary nuclear yield measurements to infer the fuel areal density and convergence, and bang times and, usually, burn durations from both DD and D^3He reactions. As will be shown, even the shock burn duration, when compared to ion diffusion times (inferred from this collection of experimental measurements), is insightful and is an excellent figure of merit for understanding the transition from hydrodynamic to strongly kinetic regimes (see Table I). It is demonstrated that standard and well-known hydrodynamic simulations [18–20] are increasingly discrepant with experimental results as the ion mean-free path becomes larger than the minimum shell radius.

A series of glass-shell implosions were performed on the OMEGA laser facility [21]. The capsules had an outer diameter of 860 ± 12 μm, a wall thickness of 2.3 ± 0.1 μm, a density of 2.15 g/cm^3, and were filled with a range of fill densities of equimolar D^3He gas, from 3.1 to 0.14 mg/cm^3. The capsules were imploded by 59 or 60 symmetrically pointed beams, delivering 14.6 kJ in a 0.6-ns pulse. Rapid laser absorption in the thin SiO_2 ablator caused a strong, spherically converging shock to be launched into the gas with a resulting Mach number of $M \sim 15$. As the shock rebounds at the center of the implosion, DD and D^3He fusion burn is initiated along the shock rebound trajectory.

For decreasing initial gas density, the Maxwellian-average mean-free path for ion-ion collisions around nuclear bang time, based on measured quantities, varied from ~40 to ~800 μm, from a regime that is reasonably hydrodynamiclike to one that is strongly kinetic. This is reflected in the Knudsen number $N_K \equiv \lambda_{ii}/R_{\text{shell}}$, the ratio of ion mean-free path to minimum shell radius, which varied from ~0.3 to 9. The Knudsen number is another figure of merit for studies of hydrodynamic and kinetic behavior. In a broader context, this near single-parameter study allows for a quantitative assessment of long mean-free-path effects in a regime comparable to the early phases of cryogenically layered hot-spot ignition implosions, in which an $M \sim 10$–50 shock converges in a DT gas of initial density 0.3 mg/cm^3 [1,22].

Radiation-hydrodynamic simulations were performed using three well-known and benchmarked hydrodynamic simulation codes: LILAC [18], HYADES [20], and DUED [19]. All three gave very similar predictions in this campaign and, as a representative case, the one-dimensional (1D) version of the two-dimensional Lagrangian DUED code [19,23] is utilized herein; it includes flux-limited electron thermal transport with a flux limiter of $f = 0.07$ and non-LTE opacities. Laser absorption is modeled by inverse bremsstrahlung with laser refraction and a 10% reduction in the input laser energy so that the time-averaged simulated absorbed laser fraction matches experimental measurements by full aperture backscatter stations [24]. Ion viscosity is included. The DUED simulation of an implosion with 1.1 mg/cm^3 D^3He is shown in Fig. 1. Lagrangian mass-element trajectories as a function of time show a rapidly converging shock, which rebounds at ~0.7 ns.

Measured DD and D^3He yields, Doppler-broadening-inferred burn-averaged ion temperatures (T_i), and DD bang

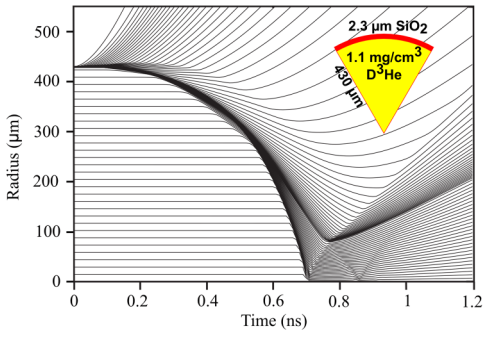

FIG. 1 (color online). Lagrangian mass-element trajectories in 1D DUED simulations [19,23] for an implosion with 1.1 mg/cm^3 D^3He. The laser pulse is a square pulse, about 0.6 ns in duration.

time, the time of peak fusion production, are compared to post-processed DUED-predicted values in Fig. 2. DD yields and burn-averaged T_i were measured using the neutron time of flight suite [25], while D^3He yields and burn-averaged T_i were measured using wedge-range-filter proton spectrometers and charged particle spectrometers [26]. The excellent agreement observed between the spectral widths of the D^3He-α and D^3He-p spectra gives a high degree of confidence in the D^3He-burn-averaged ion temperature measurement. The DD bang times were measured using the neutron temporal diagnostic [27]. Uncertainties in measured yields are $\sim \pm 10\%$, whereas the uncertainty in the DD-burn-averaged T_i is ± 0.5 keV, and the uncertainty in the D^3He-burn-averaged T_i is ± 2 keV. The absolute uncertainty in DD-neutron bang time is ± 50 ps.

DUED-simulated DD and D^3He yields are slowly varying as the initial gas density is decreased, increasing in the case of D^3He, as the decrease in density is balanced or overcome by an increase in temperature and fusion reactivity. In contrast, the measured yields decrease dramatically at low density. This discrepancy in trends is reflected in the yield over clean (YOC), the ratio of measured yields to yields simulated by 1D ("clean") hydrodynamic simulations that do not include a turbulent mix model or kinetic effects. This decrease in YOC is especially notable below ~ 1.7 mg/cm^3 and reflects the weakening confinement of fuel ions as the ion mean-free path becomes significant relative to the shell radius. Above ~ 1.7 mg/cm^3, representing a more hydrodynamiclike regime, the YOC reaches ~ 0.35 for DD and ~ 0.5 for D^3He yields.

Both the measured and DUED-simulated ion temperatures increase as gas density is decreased, suggesting that more energy is coupled to each ion at lower gas density; however, the trend in T_i is much stronger in simulation than in the experiment. Also, the difference between DD and D^3He burn-averaged ion temperatures indicates the presence of temperature gradients in the fuel, though based on the long ion-ion collision times in more strongly kinetic experiments (~ 900 ps at the lowest gas density), this difference may also partly reflect a difference in temperatures between ^3He and D ions.

The measured DD bang time is relatively independent of gas density and also matches the DUED predictions. This approximate invariance is reasonable, given that the shock decouples from the shell only ~ 300 ps before shock rebound (Fig. 1), such that the higher-velocity shock in the low-density implosion reaches the center only slightly earlier than the lower-velocity shock in the high-density implosion.

In order to qualitatively understand the strong decrease in YOC, this general trend is recast in terms of the Maxwellian-averaged ion-ion mean-free path, where $\lambda_{ii} \propto T_i^2/n_i$ [28]. As the initial fill density is decreased from 3.1 to 0.14 mg/cm^3, the ion density after shock convergence

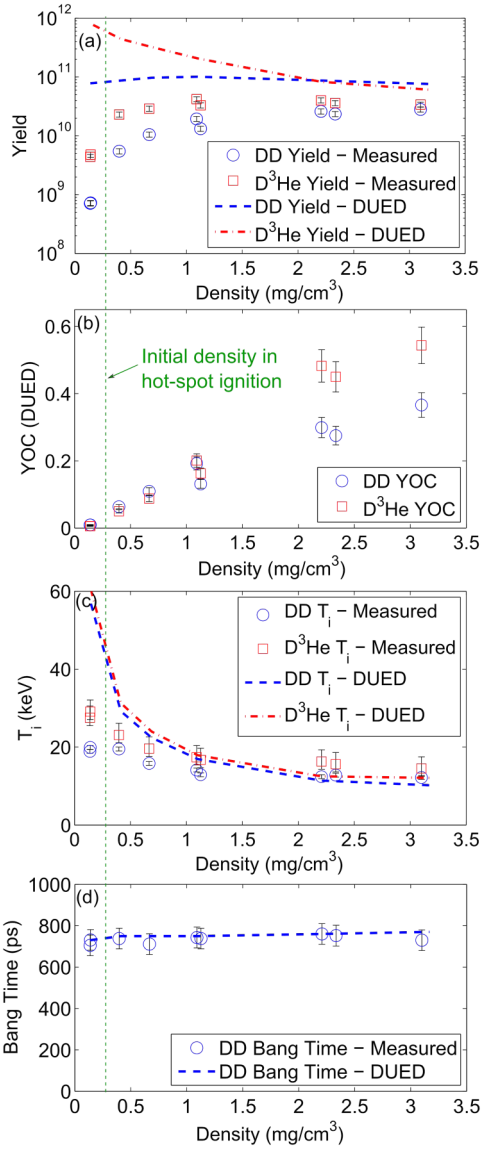

FIG. 2 (color online). Measured and DUED-simulated DD and D^3He (a) yields, (b) yields over clean (YOC) relative to DUED simulations, (c) measured and DUED-simulated burn-averaged ion temperatures, and (d) measured and DUED-simulated DD bang time as a function of initial gas density. The initial gas density in cryogenically layered ignition experiments, 0.3 mg/cm^3 [1], is indicated with the dotted vertical line. This indicates that such ignition implosions during the shock convergence phase are in the kinetic regime. Two separate experiments were performed at 0.14 mg/cm^3 with nearly identical results, indicating excellent repeatability.

decreases from $\sim 2 \times 10^{22}$ to $\sim 5 \times 10^{21}$ [29]. Concurrently with the decrease in ion density, the ion temperature (a yield-weighted average of DD- and D^3He-burn-averaged ion temperatures) increases from 14 to 28 keV, such that over the range of the experiment, λ_{ii} varies from ~ 40 μm at high density to ~ 800 μm at low density. At high density, the ion-ion mean-free path is $\sim 0.3 R_{\text{shell}}$, where R_{shell} is the x-ray-framing-camera (XRFC) [30] estimated minimum

shell radius ~130 μm. At high density, the Knudsen number $N_K \sim 0.3$, and a hydrodynamic description is more valid. At low density, $\lambda_{ii} \sim 9R_{\text{shell}}$ ($N_K \sim 9$), with $R_{\text{shell}} \sim 85$ μm, such that the hydrodynamic description is severely invalid and long ion mean-free-path effects, as reflected by the large Knudsen number, are significant (see Table I).

The DD and D^3He YOC values relative to DUED simulations [originally plotted as a function of initial gas density in Fig. 2(b)] are now shown as a function of $N_K \equiv \lambda_{ii}/R_{\text{shell}}$ in Fig. 3. Both the DD and D^3He YOC show a dramatic trend of decreasing YOC with increasing N_K, from $\text{YOC}_{\text{DD}} \sim 0.35$ and $\text{YOC}_{\text{D}^3\text{He}} \sim 0.50$ at $N_K \sim 0.3$ to $\text{YOC}_{\text{DD}} \sim 0.009$ and $\text{YOC}_{\text{D}^3\text{He}} \sim 0.006$ at $N_K \sim 9$. The hydrodynamic code does an increasingly poor job matching the measured yields as the conditions in the implosion become strongly kinetic.

In a similar vein and again based solely on experimental measurements, the ratio R_τ of the fusion burn duration to the ion diffusion time is calculated. R_τ is another figure of merit for describing hydrodynamic-kinetic regimes. The characteristic diffusion time scale based on the ion mean-free path and thermal velocity $\tau_{\text{diff}} = R_{\text{shell}}^2/((1/3)\lambda_{ii}v_{ti})$, is ~10 ps for D ions and ~40 ps for ^{3}He ions at 0.14 mg/cm^3. These diffusion times are substantially shorter than the duration of fusion burn, ~120 ps for D^3He fusion and ~140 ps for DD fusion. Conversely, in the hydrodynamiclike regime (3.1 mg/cm^3), τ_{diff} is ~600 ps for D ions and 2400 ps for ^{3}He, such that diffusion is insignificant over the duration of fusion burn, ~200 ps for DD fusion and ~160 ps for D^3He fusion. As shown in Table I, R_τ varies from ~0.3 to ~14 for DD and from ~0.07 to ~3 for D^3He fusion. Similar to the Knudsen number, R_τ reflects this transition from hydrodynamiclike to strongly kinetic. When $R_\tau \gtrsim 1$, ion diffusion must be important, and this will not be adequately accounted for in the standard hydrodynamic models.

An important issue is whether the observed YOC trend could be a result of hydrodynamic mix increasingly quenching the yield as the initial fuel density decreases,

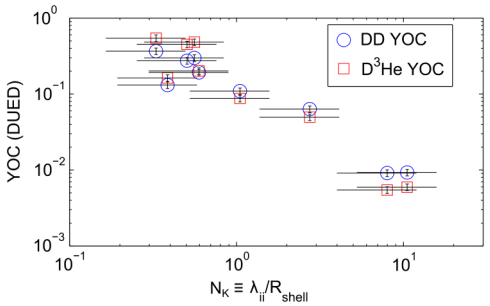

FIG. 3 (color online). YOC relative to 1D DUED simulations for both DD and D^3He reactions as a function of the Knudsen number, the ratio of the ion-ion mean-free path (at bang time) to the measured minimum shell radius.

as might well be expected in ablatively driven implosions. A fall-line analysis [31] using hydrodynamics simulations indicates that the hydrodynamic fuel-shell mix cannot substantially account for this trend, as should be expected for these low-convergence (convergence ratio ~4–5), shock-driven implosions in which there is virtually no deceleration phase [32]. Eliminating hydro-simulated yield generated outside of the radius corresponding to 20% of the distance from the fuel-shell interface to the fall-line (the maximum-velocity trajectory of the fuel-shell interface) models a near-worst-case reduction of fusion yield. This assumes that the shell is entirely mixed with the fuel in that volume and fusion reactions are completely quenched. At 3.1 mg/cm^3, the reduction in yield due to hydrodynamic mix is negligible, while even at 0.14 mg/cm^3, mix accounts for at most a factor of 2 yield reduction. Hydrodynamic mix falls short then by at least a factor of 20 in explaining the factor of 40 difference in YOC observed between 0.14 and 3.1 mg/cm^3.

As a first step to begin exploring this hydro-kinetic transition, a reduced ion kinetic (RIK) model that includes gradient-diffusion and loss-term approximations to several transport processes was implemented within a 1D radiation-hydrodynamics code [33,34]. This model includes the effects of kinetic transport of ion mass, momentum, and thermal energy and reduction in fusion reactivity owing to Knudsen-layer modification of ion-distribution tails when the ion mean-free path around bang time approaches the shell radius [16,35]. The model requires empirically determined parameters to calibrate its various flux terms. A single set of five model parameters is then constrained by the measured DD and D^3He yields, DD-burn-averaged T_i, DD bang time, and the laser absorption fraction over the entire data set (40 observables). These simulations used the nominal capsule diameter, shell thickness, and laser pulse parameters, varying only the initial fill density, as was done in the experiments. The code uses multigroup radiation diffusion, charged-fusion-product diffusion, flux-limited electron thermal diffusion ($f_e = 0.06$), and laser energy propagation via geometric ray tracing and deposition by inverse bremsstrahlung, with laser deposition and the flux limiter inferred from the observed bang time and absorption fraction.

Figure 4 shows the measured DD and D^3He yields in comparison to the RIK model and the clean hydrodynamic simulation with kinetic effects turned off. Each kinetic effect—ion thermal conduction, reactivity reduction due to Knudsen modification of the ion distribution function, and ion diffusion—has been progressively implemented to show how each effect impacts the fusion yields over the density range. The measured yield trends are captured by the full reduced ion kinetic model over the entire density range. In contrast, the clean simulation shows a very different, flat trend, similar to that in DUED simulations [Fig. 2(a)], though with slightly better agreement than

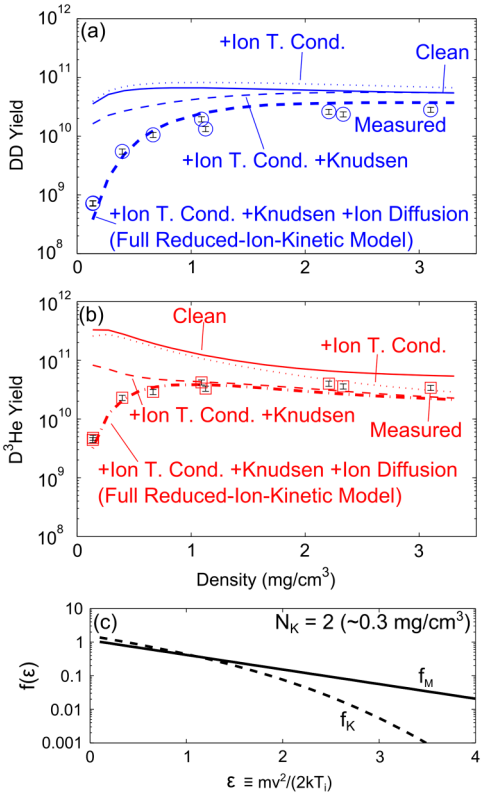

FIG. 4 (color online). Measured (a) DD and (b) D^3He yields (symbols) in comparison to the reduced ion kinetic model (thick dashed lines) and to clean hydrodynamics simulations that ignored kinetic effects (thin solid lines). Also shown are yields from simulations that progressively added ion thermal conduction (thin dotted lines) and then Knudsen reactivity reduction (thin dashed lines) onto the clean simulations, with ion diffusion also included in the full reduced ion kinetic model (thick dashed lines). The difference between the curves shows the impact each individual kinetic effect has on the yields. The (c) Knudsen-modified ion distribution function (f_K, dashed) [35], area normalized to the original Maxwellian distribution function (f_M, solid line), shows how tail ions are depleted for an average D^3He ion for a typical strongly kinetic regime (~0.3 mg/cm^3) Knudsen number of $N_K = 2$.

DUED in the high-density limit due to a lower laser absorption fraction and electron flux limiter, which produce lower clean-simulated yields.

The principal kinetic effects responsible for the reduction in yield are, first, the diffusion of ions out of the hot fuel region, which becomes especially significant at the lowest initial gas densities and, second, the reduction in fusion reactivity due to the non-Maxwellian depletion of high-energy ions. Around a density of 0.3 mg/cm^3, representative of the strongly kinetic regime, reduced fusion reactivity due to Knudsen modification of the ion distribution function is responsible for a factor of ~2.5 (~4) reduction in DD (D^3He) yield relative to the hydrodynamic model, while ion diffusion accounts for an additional factor of ~10 (~5) DD (D^3He) yield reduction. For a Knudsen number of $N_K = 2$, typical of the strongly kinetic regime around 0.3 mg/cm^3, the tail of the Knudsen-modified ion distribution function is significantly depleted relative to the corresponding Maxwellian ion distribution function, especially for normalized ion energies $\epsilon \equiv mv^2/2kT_i > 2$. As the fusing reactant ions typically have energies well above the thermal energy, this depletion of high-energy ions due to long mean-free paths can have a large impact on the fusion reactivity.

To summarize, a systematic and comprehensive set of experiments using shock-driven D^3He implosions, in which a wide array of diagnostics were employed, has demonstrated a dramatically increasing yield deficit, relative to hydrodynamic predictions, with decreasing initial gas density. This study methodically varied the Knudsen number from 0.3 to 9, or the ratio of the fusion burn duration to the ion diffusion time R_τ, from ~0.3 to ~14. Both dimensionless parameters, directly inferred from experimental measurements, indicate the degree of ion kinetic effects. Hydrodynamic mix cannot account for these observations. As a step towards illuminating the role of ion kinetic effects, a model requiring empirically calibrated parameters for determining the flux terms is utilized. This model incorporates ion transport and deviations from Maxwellian behavior within the framework of a radiation-hydrodynamics simulation, and it effectively captures the measured yield trends. In a broader context, an important question concerns the potential role of kinetic effects in the evolution of ignition implosions at the National Ignition Facility [1]. Could the shock convergence phase, which mirrors low-density, shock-driven implosions discussed herein, impact the subsequent evolution of the compressional phase of the implosion, which is highly collisional and hydrodynamic in nature? It is possible that insight into this question could be culled by measuring, with high accuracy, the differential as well as the absolute timing of both shock and compression bang times in surrogate ignition capsules filled with D^3He [36], as is being planned [37,38], and contrasting these measurements to the predictions of hydrodynamic simulations used at the National Ignition Facility.

The authors thank R. Frankel and E. Doeg for contributing to the processing of the CR-39 data used in this work as well as the OMEGA operations crew for their help in executing these experiments. This work is supported in part by US DOE (Grants No. DE-NA0001857 and No. DE-FC52-08NA28752), FSC (No. 5-24431), NLUF (No. DE-NA0002035), LLE (No. 415935-G), and LLNL (No. B597367). S.A. is supported by Italian Grants No. PRIN 2009FCC9MS and No. Sapienza 2012 C26A12CZH2.

*mrosenbe@mit.edu

[1] M. J. Edwards *et al.*, Phys. Plasmas **20**, 070501 (2013).
[2] T. R. Dittrich *et al.*, Phys. Rev. Lett. **112**, 055002 (2014).

[3] T. C. Sangster *et al.*, Phys. Plasmas **20**, 056317 (2013).
[4] S. Atzeni and J. Meyer-Ter-Vehn, *The Physics of Inertial Fusion: Beam Plasma Interaction, Hydrodynamics, Hot Dense Matter*, International Series of Monographs on Physics (Oxford University Press, New York, 2004).
[5] J. Lindl, Phys. Plasmas **2**, 3933 (1995).
[6] J. R. Rygg, J. A. Frenje, C. K. Li, F. H. Séguin, R. D. Petrasso, F. J. Marshall, J. A. Delettrez, J. P. Knauer, D. D. Meyerhofer, and C. Stoeckl, Phys. Plasmas **15**, 034505 (2008).
[7] J. R. Rygg *et al.*, Phys. Plasmas **13**, 052702 (2006).
[8] D. T. Casey *et al.*, Phys. Rev. Lett. **108**, 075002 (2012).
[9] H. W. Herrmann *et al.*, Phys. Plasmas **16**, 056312 (2009).
[10] P. Amendt, O. L. Landen, H. F. Robey, C. K. Li, and R. D. Petrasso, Phys. Rev. Lett. **105**, 115005 (2010).
[11] G. Kagan and X.-Z. Tang, Phys. Plasmas **19**, 082709 (2012).
[12] C. Bellei, P. A. Amendt, S. C. Wilks, M. G. Haines, D. T. Casey, C. K. Li, R. Petrasso, and D. R. Welch, Phys. Plasmas **20**, 012701 (2013).
[13] O. Larroche, Eur. Phys. J. D **27**, 131 (2003).
[14] O. Larroche, Phys. Plasmas **19**, 122706 (2012).
[15] D. Li, V. N. Goncharov, I. V. Igumenshchev, and S. Skupsky, Bull. Am. Phys. Soc. **52**, 11 (2007).
[16] K. Molvig, N. M. Hoffman, B. J. Albright, E. M. Nelson, and R. B. Webster, Phys. Rev. Lett. **109**, 095001 (2012).
[17] A. G. Petschek and D. B. Henderson, Nucl. Fusion **19**, 1678 (1979).
[18] J. Delettrez, Can. J. Phys. **64**, 932 (1986).
[19] S. Atzeni, Comput. Phys. Commun. **43**, 107 (1986).
[20] J. T. Larsen and S. M. Lane, J. Quant. Spectrosc. Radiat. Transfer **51**, 179 (1994).
[21] T. R. Boehly *et al.*, Opt. Commun. **133**, 495 (1997).
[22] J. D. Lindl, P. Amendt, R. L. Berger, S. G. Glendinning, S. H. Glenzer, S. W. Haan, R. L. Kauffman, O. L. Landen, and L. J. Suter, Phys. Plasmas **11**, 339 (2004).
[23] S. Atzeni, A. Schiavi, F. Califano, F. Cattani, F. Cornolti, D. Del Sarto, T. Liseykina, A. Macchi, and F. Pegoraro, Comput. Phys. Commun. **169**, 153 (2005).
[24] W. Seka, H. A. Baldis, J. Fuchs, S. P. Regan, D. D. Meyerhofer, C. Stoeckl, B. Yaakobi, R. S. Craxton, and R. W. Short, Phys. Rev. Lett. **89**, 175002 (2002).
[25] V. Y. Glebov, C. Stoeckl, T. C. Sangster, S. Roberts, G. J. Schmid, R. A. Lerche, and M. J. Moran, Rev. Sci. Instrum. **75**, 3559 (2004).
[26] F. H. Séguin *et al.*, Rev. Sci. Instrum. **74**, 975 (2003).
[27] C. Stoeckl, V. Y. Glebov, S. Roberts, T. C. Sangster, R. A. Lerche, R. L. Griffith, and C. Sorce, Rev. Sci. Instrum. **74**, 1713 (2003).
[28] The ion-ion mean-free path used throughout is the geometric mean of D and ^{3}He mean-free paths, inferred from measured quantities.
[29] The ion density is inferred either from the fuel ρR as measured by the ratio of secondary DT-neutron yield to primary DD-neutron yield [39] or from the minimum shell radius as estimated from XRFC images [30]. The decrease in initial gas density is offset partially by an increase in shell convergence, though convergence effects and the significance of hydrodynamic instabilities and mix is, as will be shown, minimal.
[30] D. K. Bradley, P. M. Bell, O. L. Landen, J. D. Kilkenny, and J. Oertel, Rev. Sci. Instrum. **66**, 716 (1995).
[31] P. Amendt, J. D. Colvin, R. E. Tipton, D. E. Hinkel, M. J. Edwards, O. L. Landen, J. D. Ramshaw, L. J. Suter, W. S. Varnum, and R. G. Watt, Phys. Plasmas **9**, 2221 (2002).
[32] In the deceleration phase of ablatively driven implosions, Rayleigh-Taylor instabilities can introduce substantial mix, degrading implosion performance and reducing fusion yields.
[33] N. Hoffman *et al.*, Bull. Am. Phys. Soc. **58**, 16 (2013).
[34] A different approach to analyzing the data of Fig. 2(a), based on a hybrid kinetic-Guderley model, has recently been reported by Amendt *et al.* [40].
[35] B. J. Albright, K. Molvig, C.-K. Huang, A. N. Simakov, E. S. Dodd, N. M. Hoffman, G. Kagan, and P. F. Schmit, Phys. Plasmas **20**, 122705 (2013).
[36] D. G. Hicks *et al.*, Phys. Plasmas **19**, 122702 (2012).
[37] A. B. Zylstra *et al.*, Rev. Sci. Instrum. **83**, 10D901 (2012).
[38] H. G. Rinderknecht *et al.*, Rev. Sci. Instrum. **83**, 10D902 (2012).
[39] M. D. Cable and S. P. Hatchett, J. Appl. Phys. **62**, 2233 (1987).
[40] P. Amendt, C. Bellei, S. Wilks, C. Li, H. Rinderknecht, M. Rosenberg, H. Sio, and R. Petrasso, Bull. Am. Phys. Soc. **58**, 16 (2013).